New Age of Polymer Nanocomposites Containing Dispersed High-Aspect-Ratio Silicate Nanolayers

Kenji Tamura,*,† Shingo Yokoyama,‡ Chelo S. Pascua,† and Hirohisa Yamada†

Photocatalytic Material Center, National Institute for Materials Science 1-1 Namiki, Tsukuba, Ibaraki 305-0044, Japan, and Civil Engineering Research Laboratory, Central Research Institute of Electric Power Industry, 1646 Abiko, Abiko, Chiba 270-1194, Japan

Received October 4, 2007. Revised Manuscript Received January 10, 2008

A new natural mica/epoxy nanocomposite was formed through the exfoliation of a mica layer. The natural mica used was a potassium sericite (K-SE) whose interlayer was saturated with potassium cations. Powdered samples were separated through an air classifier into $D_{50} = 13.6$ μm (its median particle diameter), $D_{10} = 7.9$ μm, and $D_{90} = 23.7$ μm. An organophilic SE was prepared by an ion exchange reaction between the SE powder and alkylammonium solutions of various initial concentrations. As a typical procedure to forming a completely organically modified sample, the K-SE powder was treated with the highest alkylammonium concentration. This corresponded to an alkylammonium$^+$/K$^+$ mole ratio = 10.0 which was kept at 90 °C for four days. The nanocomposites were prepared by dispersing the organophilic SE in an epoxy resin (diglyxidyl ether of bisphenol A, DGEBA) with subsequent curing in the presence of nadic methyl anhydride (NMA) and benzyldimethylamine (BDMA) at 120–180 °C. Considerable exfoliation of the organically modified SE was achieved at a curing temperature of 180 °C. The morphology of the nanocomposite showed silicate nanolayers with extremely high aspect ratios that are at levels several dozens to hundreds of times greater than that of conventional exfoliated clay−polymer nanocomposites.

Introduction

The new technological field in polymer−clay nanocomposite materials has received increased attention since the 1990s. Several researchers use a layer-by-layer assembly technique[1–5] to accomplish the desired polymer−clay nanocomposite properties. In this study, we opted to use polymer nanocomposites with dispersed clay nanolayers. Following the pioneering work of Toyota researchers who demonstrated the first practical application of a clay−polyamide 6 nanocomposite in the automobile industry,[6] numerous researchers have reported the preparation of exfoliated clay−polymer nanocomposites in various polymer systems, such as polyimides,[7,8] epoxies,[9–17] elastomers,[18–20] polypropylene,[21–25] polyester,[26,27] polydimethylsiloxane,[28] polylactide,[29–31] and

* To whom all correspondence should be addressed. E-mail: tamura.kenji@nims.go.jp.
† National Institute for Materials Science.
‡ Central Research Institute of Electric Power Industry.

(1) Kleinfeld, E. R.; Ferguson, G. S. *Science* **1994**, *265*, 370–373.
(2) Lvov, Y.; Ariga, K.; Ichinose, I.; Kunitake, T. *Langmuir* **1996**, *12*, 3038–3044.
(3) Ogata, Y.; Kawamata, J.; Chong, C.-H.; Yamagishi, A.; Saito, G. *Clays Clay Miner.* **2003**, *51*, 181–185.
(4) Podsiadlo, P.; Kaushik, A. K.; Arruda, E. M.; Waas, A. M.; Shim, B. S.; Xu, J.; Nandivada, H.; Pumplin, B. G.; Lahann, J.; Ramamoorthy, A.; Kotov, N. A. *Science* **2007**, *318*, 80–83.
(5) Rouse, J. H.; Ferguson, G. S. *Clays Clay Miner.* **2007**, *55*, 160–164.
(6) (a) Fukushima, Y.; Okada, A.; Kawasumi, M.; Kurauchi, T.; Kamigaito, O. *Clay Miner.* **1988**, *23*, 27–34. (b) Kurauchi, T.; Okada, A.; Nomura, T.; Nishio, T.; Saegusa, S.; Deguchi, R. *SAE Technical Paper* **1991**, *910584*, 1–7. (c) Usuki, A.; Kawasumi, M.; Kojima, Y.; Okada, A.; Kurauchi, T.; Kumigaito, O. *J. Mater. Res.* **1993**, *8*, 1174–1178. (d) Usuki, A.; Kawasumi, M.; Kojima, Y.; Fukushima, Y.; Okada, A.; Kurauchi, T.; Kumigaito, O. *J. Mater. Res.* **1993**, *8*, 1179–1184. (e) Kojima, Y.; Usuki, A.; Kawasumi, M.; Okada, A.; Kurauchi, T.; Kumigaito, O. *J. Polym. Sci. Part A., Polym. Chem.* **1993**, *31*, 983–986. (f) Kojima, Y.; Usuki, A.; Kawasumi, M.; Okada, A.; Kurauchi, T.; Kumigaito, O. *J. Appl. Polym. Sci.* **1993**, *49*, 1259–1264.
(7) Yano, K.; Usuki, A.; Okada, A. *J. Polym. Sci., Part A: Polym. Chem.* **1997**, *35*, 2289–2294.
(8) Orasa, K.; Rathanawan, M.; Johannes, W. S. *J. Appl. Polym. Sci.* **2003**, *89*, 2875–2881.
(9) Messersmith, P. B.; Giannelis, E. P. *Chem. Mater.* **1994**, *6*, 1719–1725.
(10) Wang, M. S.; Pinnavia, T. J. *Chem. Mater.* **1994**, *6*, 468–474.
(11) Lan, T.; Kaviratna, D.; Pinnavaia, T. J. *J. Phys. Chem. Solids* **1996**, *57*, 1005–1010.
(12) Wang, Z.; Massam, J.; Pinnavaia, T. J. In *Polymer-clay nanocomposites*; Pinnavaia, T. J., Beall, G. W., Eds.; Wiley series in polymer science; Wiley: New York, 2000; pp 127–149.
(13) Kornmann, X.; Lindberg, H.; Berglund, L. A. *Polymer* **2001**, *42*, 1303–1310.
(14) Chin, I. J.; Thurn-Albrecht, T.; Kim, H. C.; Russell, T. P.; Wang, J. *Polymer* **2001**, *42*, 5947–5952.
(15) Triantafillidis, C. S.; LeBaron, P. C.; Pinnavaia, T. J. *J. Solid State Chem.* **2002**, *167*, 354–362.
(16) Koerner, H.; Jacobs, D.; Tomlin, D. W.; Busbee, J. D.; Vaia, R. D. *Adv. Mater.* **2004**, *16*, 297–302.
(17) Ma, J.; Yu, Z. Z.; Zhang, Q. X.; Xie, X. L.; Mai, Y. W.; Luck, I. *Chem. Mater.* **2004**, *16*, 757–759.
(18) Wang, Z.; Pinnavaia, T. J. *Chem. Mater.* **1998**, *10*, 3769–3771.
(19) Usuki, A.; Tukigase, A.; Kato, M. *Polymer* **2002**, *43*, 2185–2189.
(20) Lee, H. S.; Fasulo, P. D.; Rodgers, W. R.; Paul, D. R. *Polymer* **2005**, *46*, 11673–11689.
(21) Hasegawa, N.; Kato, M.; Usuki, A.; Okada, A. *Macromolecules* **1997**, *30*, 6333–6338.
(22) Hasegawa, N.; Kawasumi, M.; Kato, M.; Usuki, A.; Okada, A. *J. Appl. Polym. Sci.* **1998**, *67*, 87–92.
(23) Garcés, J. M.; Moll, D. J.; Bicerano, J.; Fibiger, R.; MacLeod, D. G. *Adv. Mater.* **2000**, *12*, 1835–1839.
(24) Xiaohui, L.; Qiuju, W. *Polymer* **2001**, *42*, 10013–10019.
(25) Sun, T.; Garcés, J. M. *Adv. Mater.* **2002**, *14*, 128–130.
(26) Tsai, T. Y. In *Polymer-clay nanocomposites*; Pinnavaia, T. J., Beall, G. W., Eds.; Wiley series in polymer science; Wiley, New York: 2000; pp 173–189.

10.1021/cm702860m CCC: $40.75
Published on Web 03/04/2008

hydrogels.[32] More often than not, the clay (layer silicate) component of conventional polymer nanocomposites is a smectite (montmorillonite). In an "exfoliated clay−polymer nanocomposite" the clay component's layers are individually dispersed in the polymer matrix. The resulting nanocomposite exhibits high tensile strength, modulus, heat distortion temperature, and excellent barrier properties at low clay contents. It is interesting to understand the factors underlying this high performance. Numerous reports have identified the dispersed clay's aspect ratio (lateral length/thickness ratio) as a key influence of this improvement.[6,34] An individual clay nanolayer has its highest possible aspect ratio in its fully exfoliated state. In particular, Fornes and his co-workers have estimated the average aspect ratio to be ∼70 for the exfoliated montmorillonite (clay) layers in an extruded clay−polyamide 6 nanocomposite.[33,34] This is a remarkably large value in comparison with composites that are reinforced with conventional glass fiber and other minerals. They further confirmed the correlation between the aspect ratio and the modulus of the composite in well-exfoliated clay−polymer nanocomposites in accordance with classical composite theory.[35] To achieve further improvements in nanocomposite properties through an increase in aspect ratios, new layered materials with higher aspect ratios are needed besides the commonly used clay.

Most reviews have dealt with layered silicate−polymer nanocomposites based on smectite clays. Studies on other types of layered silicate−polymer nanocomposite have been conducted to a much lesser degree because of the relatively greater difficulty in preparing polymer-intercalated compounds. Natural micas are ubiquitous in nature and can be obtained in their mineralogically pure form at a low cost. The net negative layer charge of mica layers is balanced by interlayer K^+ ions (Figure 1). These ions are not exchangeable because they are strongly bound to interlayer surfaces in the form of inner-sphere complexes. For this reason, mica do not expand in water.[36,37] Therefore, despite their high crystallinity and large particle size (over several dozen times that of clay particles), they have never been used in nanocomposites because of their "non-expandability". To our knowledge, no one has attempted their use due to firmly held notions about this nonexpandability or "difficult ion-exchangeability". If natural micas were fully exfoliated,

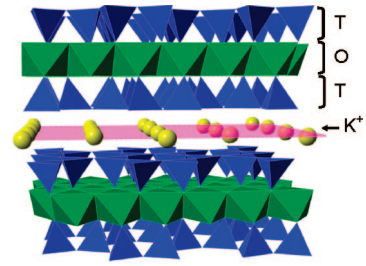

Figure 1. Structure of mica viewed approximately perpendicular to the *c* axis. The mica structure consists of sheets of tetrahedra (T) arranged in pairs, enclosing, sandwich-fashion, a sheet of edge-sharing octahedra (O). The apexes of the tetrahedra connect to the octahedra of the central layer. Between each "sandwich", there are interlayer sites which can contain large cations, for example, potassium (K^+).

Scheme 1. Comparing the Dimension of Silicate Nanolayers Derived from (a) Smectites (Clay) and (b) Mica

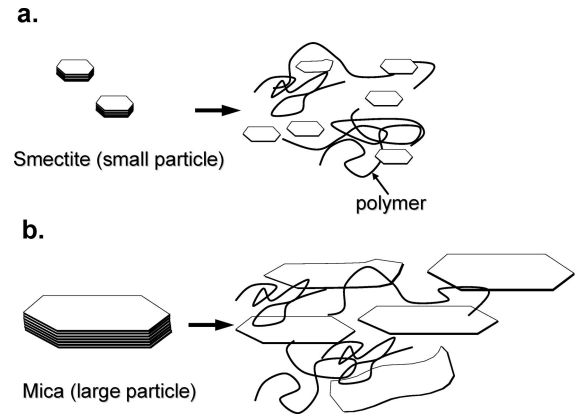

however, the aspect ratio of individual layers would greatly exceed that of smectites. The performance of the resulting nanocomposite would, therefore, be superior to that of their conventional counterparts (Scheme 1).

Mackintosh et al. have reported on the weathering of micas whose interlayer potassium cations (natural mica) had been replaced slowly with organic cations through a treatment with a highly concentrated alkylammonium salt solution.[38] The preparation of suitable organophilic mica compounds in this study has laid the foundation for the synthesis of layered silicate−polymer nanocomposites containing layers with large aspect ratios. In this paper, we report the preparation of organophilic mica particles based on the natural sericite (SE, Figure 2) that has a median diameter of 13.6 μm through treatment with concentrated alkylammonium species. We also report our attempts to prepare the first exfoliated natural mica−epoxy nanocomposite.

Experimental Section

Sample Preparation. The natural mica is a potassium sericite (K-SE) mined in a hydrothermal deposit in Shimane, Japan. Its composition is $(K_{0.77}Na_{0.03})(Al_{1.67}Fe^{2+}_{0.18}Mg_{0.10})(Si_{3.24}Al_{0.76})O_{10}(OH)_2$. Its cation exchange capacity determined is 203 mequiv/100 g. The powdered sample was separated through a zigzag-type air-classifier (Multi Processing System 100 AFG, Hosokawa Micron) into D_{50} = 13.6 μm (median particle diameter), D_{10} = 7.9

(27) Matayabas, J. C., Jr; Turner, S. R. In *Polymer-clay nanocomposites*; Pinnavaia, T. J., Beall, G. W., Eds.; Wiley series in polymer science; Wiley: New York, 2000; pp 207–225.
(28) Burnside, S. D.; Giannelis, E. P. *Chem. Mater.* **1995**, *7*, 1597–1600.
(29) Maiti, P.; Yamada, K.; Okamoto, M.; Ueda, K.; Okamoto, K. *Chem. Mater.* **2002**, *14*, 4654–4661.
(30) Ray, R. R.; Maiti, P.; Okamoto, M.; Yamada, K.; Ueda, K. *Macromolecules* **2002**, *35*, 3104–3110.
(31) Ray, S. S.; Yamada, K.; Okamoto, M.; Fujimoto, Y.; Ogami, A.; Ueda, K. *Polymer* **2003**, *44*, 6633–6646.
(32) Haraguchi, K.; Takehisa, T. *Adv. Mater.* **2002**, *14*, 1120–1124.
(33) Fornes, T. D.; Paul, D. R. *Polymer* **2003**, *44*, 4993–5013.
(34) Fornes, T. D.; Hunter, D. L.; Paul, D. R. *Polymer* **2004**, *45*, 2321–2331.
(35) Halpin, J. C.; Kardos, J. L. *Polym. Eng. Sci.* **1976**, *16*, 344–352.
(36) van Olphen, H. *An Introduction to Clay Colloid Chemistry: for clay technologists, geologists, and soil scientists*; John Wiley & Sons: New York, 1977; pp 57–82.
(37) Giese, R. F., Jr. In *Micas: Reviews in Mineralogy*; Bailey, S. W., Ed.; Mineralogical Society of America, BookCrafters: Chelsea, MI, 1987; Vol. 13, pp 105–144.
(38) Mackintosh, E. E.; Lewis, D. G.; Greenland, D. J. *Clays Clay. Miner.* **1971**, *19*, 209–218.

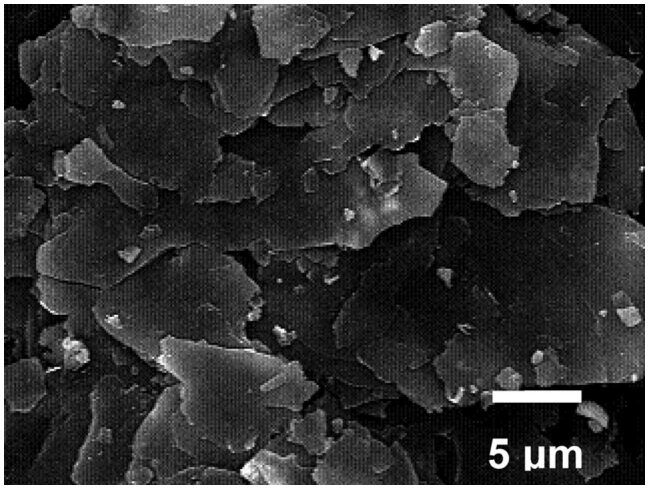

Figure 2. SEM micrograph of the separated sericite powder.

μm, and $D_{90} = 23.7$ μm, where D_{10} and D_{90} represent cumulative diameters of 10% and 90%, respectively.

Dodecylamine (DDA) and octadecylamine (ODA) hydrochloride were obtained from Wako Pure Chemical Industries, Japan, and used as received. The DDA-SE was prepared by an ion exchange reaction between SE and DDA solutions of various initial concentrations (7.3, 14.7, 21.9, 36.7, and 73.3 mM, corresponding to DDA^+/K^+ mole ratios = 1.0, 2.0, 3.0, 5.0, and 10.0, respectively). In a typical procedure, 0.3 g of SE powder was treated with 100 mL of a DDA solution and kept at 90 °C for four days. The resulting organically modified sericites (SE) were designated as DDA-SE and ODA-SE, respectively.

The dried organically modified mica powder was added with stirring to diglycidyl ether of bisphenol A (DGEBA, Japan Epoxy Resins' EPIKOTE 828, epoxy equivalent weight = 190 g/equiv) and cured with either methyl nadic anhydride (MNA, Wako Pure Chemical) or benzyldimethylamine (BDMA, Aldrich). The amount of curing agent used was DGEBA/MNA: 87.5 parts of MNA/hundred resin (phr), with 1.5 phr BDMA. Organophilic SE/DGEBA mixtures were kneaded with a three-roll mill (DR-35, Kaneda Scientific) at room temperature and then stirred at 90 °C for 1 h. After the samples were cooled, the curing agent was added with thorough mixing, and the mixture was loaded into 50-mL centrifuge tubes. Samples were centrifuged for 30 s at 3000 rpm to remove bubbles and then cast as 0.2-mm-thick films. Samples were cured for 6 h at 120, 150, and 180 °C. The mica loading of the nanocomposites prepared was 4 wt % on a silicate basis.

Characterization. Total elemental analyses of the original SE and the organically modified SE samples were performed with an inductively coupled plasma−optical emission spectrometer (ICP-OES) (IRIS Advantage, Nippon Jarrell-Ash). The concentrations of Na, K, Fe, and Mn were determined by dissolving a 20 mg of sample in 1 mL of H_2SO_4 (1 + 1) and 1 mL of HF. The mixture was heated at 200 °C until dry. The cooled residue was redissolved by adding 1 mL of HCl and pure water under ultrasonication. For determination of Si, Al, Mg, Ti, and Ca content, 20 mg samples were molten with 0.5 g of Na_2CO_3 and 0.2 g of H_3BO_3 at 1000 °C. The cooled glass was dissolved by ultrasonication in a mixture of 2 mL of HCl and pure water. These aqueous solutions were used in the elemental analysis by ICP-OES. The final amounts of interlayer K^+ in the samples were estimated based on the composition of the silicate framework.

X-ray diffraction (XRD) data were collected with a Rigaku RINT2000 XRD spectrometer with graphite monochromatized Cu Kα radiation ($\lambda = 0.154$ nm). Scan speed and step size used were 2°/min at 0.02°, respectively. Quartz was used as a calibration standard. Transmission electron microscopy (TEM) was performed on samples extracted from the film specimens. Ultrathin sections, approximately 90 nm in thickness, were cryogenically cut in the plane comprised of the cross section of the film specimen using a PT-XL ultramicrotome with an RMC Products CR-X Cryosectioning System (Boeckeler Instruments, Inc.). The resulting sections were placed on Cu grids and subsequently viewed with a JEOL 1010 electron microscope operating at 100 kV.

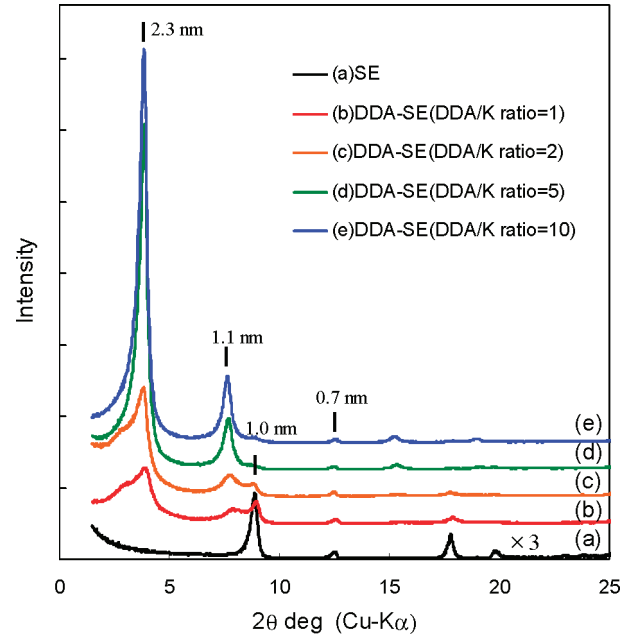

Figure 3. X-ray diffraction patterns of sericite (SE) and dodecylamine modified sericite (DDA-SE) prepared by ion exchange with different initial DDA concentrations at 90 °C for 4 days.

Results and Discussion

Figure 3 shows XRD profiles of pristine SE and the DDA-SE compounds treated with solutions of different initial DDA concentrations (DDA^+/K^+ mole ratios = 1.0, 2.0, 5.0, and 10.0; K^+ is the interlayer cation of SE) at 90 °C for four days (see Experimental Section). The intercalation reaction reached an equilibrium state on the fourth day. The XRD profile of pristine SE powder (a) shows the primary unexpanded silicate (001) reflection at 8.8° corresponding to a (widely quoted) monolayer thickness of 1.0 nm. The XRD profile of SE treated with DDA^+/K^+ mole ratio = 1.0 (b), 2.0 (c), 5.0 (d), and 10.0 (e) have corresponding peaks at 2.3 nm, 1.1 nm, 1.0, and 0.7 nm. The 2.3 and 1.1 nm peak corresponds to the $d(00l)$ reflections. Faint peaks at 2θ values of ~8.8° and ~12.3° are unexpanded phases of sericite, and a kaolin impurity, respectively. The highest concentration of DDA^+ applied to the SE has a d_{001} peak at 2.3 nm and arises from the arrangement of interpenetrating monolayers of alkylammonium ions attached to opposite silicate surfaces.[39] The intensity of the 2.3 nm peak increases with the DDA^+/K^+ mole ratio suggesting that intercalation is directly influenced by the concentration of alkylammonium solution. This is further collaborated by the decrease of XRD peak intensity for the unexpanded phase ($d_{001} = 1.0$ nm) with an

(39) Walker, G. F. *Clays Clay. Miner.* **1967**, *7*, 129–143.

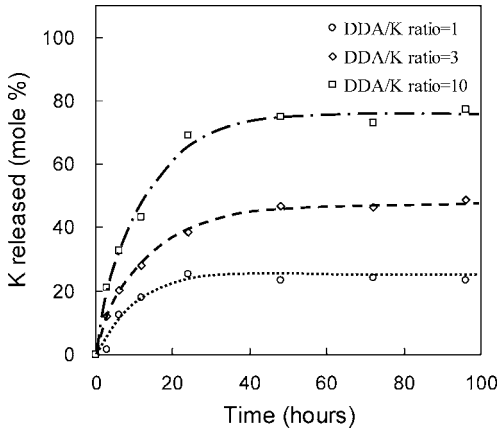

Figure 4. Effect of initial DDA concentration on the displacement of potassium from sericite (SE).

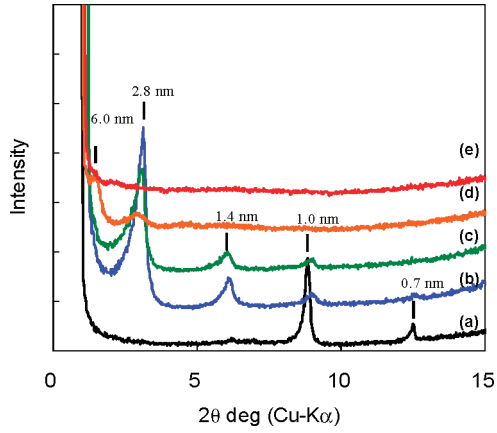

Figure 5. XRD patterns of cured SE/DGEBA/MNA (a), uncured DDA-SE/DGEBA mixture (b), and DDA-SE/DGEBA/MNA heated at various temperatures for 6 h: (c) 120 °C, (d) 150 °C, (e) 180 °C. The sericite loading was 4 wt % on silicate basis.

increase in DDA^+ concentration (Figure 3a−e). The rate of potassium release from SE in solutions after exchange reactions also increased with DDA^+ concentration (Figure 4). Upon using a $DDA^+/K^+ = 10.0$, the SE sample reached its plateau region after 48 h displacing nearly 75% of its potassium content prior to final equilibration. Compared to Na-montmorillonite, this is an extremely slow rate of exchange reaction. A nanocomposite was prepared utilizing the final phase of the intercalated compounds (i.e., fully loaded with alkylammonium ions). ODA-SE that was treated with ODA concentrations of $ODA^+/K^+ = 5.0$ under similar conditions exhibited a 3.4-nm basal spacing.

XRD analysis was also used to follow the progressive exfoliation of organophilic SE upon mixing with diglycidyl ether of bisphenol A (DGEBA) and subsequent curing. The progressive change in the XRD profile of the DDA-SE/DGEBA mixture (after stirring at 90 °C for 1 h) and of the composites cured by addition of either methyl nadic anhydride (MNA) or benzyldimethylamine (BDMA) followed by treatment for 6 h at temperatures up to 180 °C is shown in Figure 5. In a conventional SE-reinforced composite (Figure 5 a), a *d*(001) reflection of 1 nm was observed. XRD profiles for the DDA-SE/DGEBA mixture with MNA and BDMA at various intervals from room temperature to 180 °C are represented in b−e. At room temperature (b) and at 120 °C

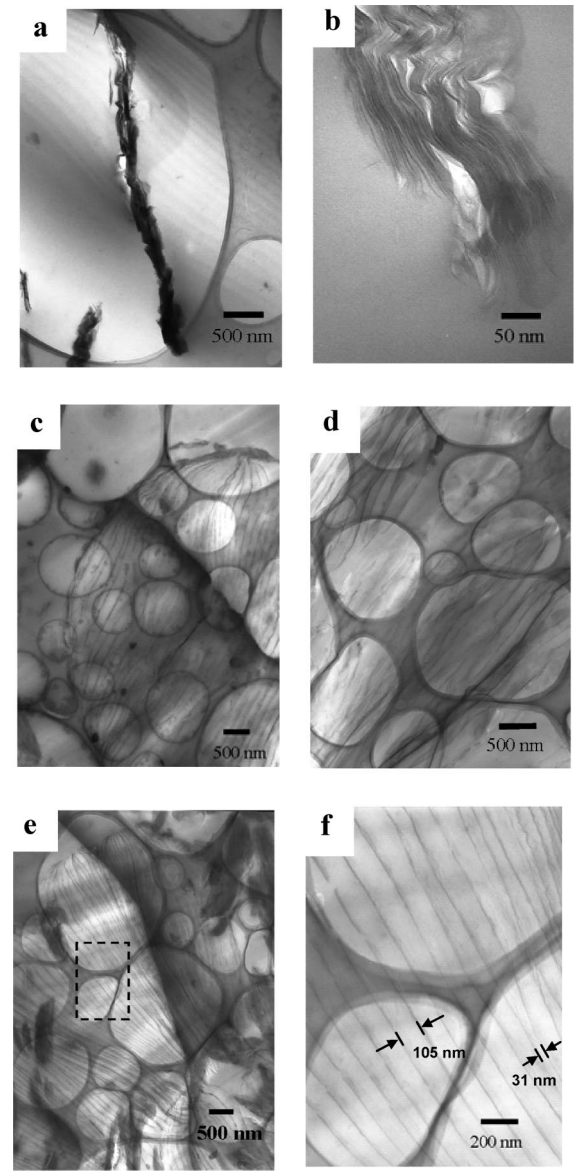

Figure 6. TEM images of thin sections of glassy epoxy composites: SE/epoxy system cured at 150 °C for 6 h (a), DDA-SE/epoxy system cured at 120 °C for 6 h (b), DDA-SE/epoxy system cured at 180 °C for 6 h (c), ODA-SE/epoxy system cured at 180 °C for 6 h (d), another image of the same (e), and the rectangular region marked in part e at high magnification (f). The sericite loading was 4 wt % on a silicate basis.

(c), expansion in the XRD profiles from 2.3 to 2.8 nm indicates the intercalated structure of DDA-SE/Epoxy. The basal spacing did not increase beyond 2.8 nm with temperatures up to 120 °C. Upon increasing the curing temperature to 150 °C, a gradual increase in *d* spacing from 2.8 nm to approximately 6 nm was observed in part d. This peak almost disappeared at 180 °C (e). The virtual disappearance of the *d*(001) reflections in DDA-SE strongly suggested the delamination of DDA-SE layers.

Figure 6 shows TEM images of epoxy/SE cured at 150 °C for 6 h (a); DDA-SE/epoxy cured at 120 °C for 6 h (b); epoxy/DDA-SE cured at 180 °C for 6 h (c); and ODA-SE/epoxy cured at 180 °C for 6 h (d, e). The dark areas represent the silicate layers while the gray/white areas are the epoxy matrix. An ultrathin section of the epoxy composite containing pristine sericite after curing at 120 °C for 6 h is shown

by Figure 6 a. The image shows a rather rigid SE platelet (cross section) in the epoxy matrix with a cross-sectional length of about 5 μm and a thickness of ~200 nm. The DDA-SE/epoxy cured at 120 °C for 6 h (Figure 6 b) indicates that the DDA-SE layers did not occupy the entire composite volume since large regions of pure epoxy matrix remain visible. At a higher magnification, each dark line corresponds to stacked wavy layers at intervals of about 2–3 nm. After curing at 180 °C for 6 h, DDA-SE layers were observed as just starting to delaminate (Figure 6 c). It can be seen clearly in Figure 6 d,e that ODA-SE was thoroughly dispersed in the ODA-SE/epoxy nanocomposite matrix.

The TEM images have shown that stacked layers of SE start to delaminate after treatment at 180 °C for 6 h. Highly ordered exfoliated structures were observed in the matrix with interlayer distances that range from several tens of nanometers to around 100 nm (Figure 6 c–f). Several expanded micrometer-sized SE platelets show onion-like structures in its exfoliation (Figure 6 c). It was quite evident from the micrographs that epoxy molecules were polymerized in the gallery region of the mica. Well-dispersed individual silicate layers (dark lines) are also found (Figure 6 d). The nanolayer thickness of approximately 2–3 nm deduced from the TEM images is thicker than a single silicate layer which could have been caused by tilted layers inclined obliquely to the sectioned plane. Despite the thicker dimension, it was clearly shown that exfoliation has taken place. Another image shows the same sample in Figure 6 e. Here, the silicate layers have a 1-nm thickness with lengths that exceed more than 5 μm deeply embedded in the epoxy matrix. At higher magnifications (Figure 6 f), the large SE nanolayers shown in the previous figure display streaks of dark lines which are cross sections of the delaminated organophilic SE monolayers in epoxy. The dispersed nanolayers obtained in this study have a lateral size greater than 5 μm (Figure 6 d,e) producing a very large aspect ratio (ca. several thousands larger) that were better defined than smectite nanolayers reported so far.[33,34] Particle sizes of SE used in this study have a median diameter of 13.6 μm and also include larger particles whose D_{90} diameter was more than 20 μm. XRD patterns of the nanocomposite cured at 180 °C for 6 h showed that all sericite particles were exfoliated and dispersed homogeneously in the epoxy matrix.

A curing agent (MNA) that would either cross-link DGEBA in the presence of organo-SE or catalyze the cross-linking reaction between organo-SE and DGEBA was used. Protonated primary amine cations on exchanged sites of the silicate could act as an acid catalyst rather than a curing agent.[10] The complete sequence of delamination has not yet been determined, although one strong possibility involves a reaction of protonated primary amine cations in the SE interlayer as a catalyst with MNA to form the monoester.[40] A nascent carboxylic group of the monoester could react with the epoxide resulting in the formation of the diester.[9] A further reaction of diester with DGEBA would result in epoxy network formation. This reaction sequence that takes place within the interlayer results in a delamination of the SE layers. XRD data clearly show that DDA-SE began to exfoliate at a curing temperature of 150 °C (Figure 5). The larger particle size and layer charge of natural SE compared to smectites implied a strong attraction between silicate layers and consequently a lower activity of the interlayer, which is reflected on the unchanged 00*l* reflections of DDA-SE at 120 °C. Although further work is required to verify the reaction pathway involved, it is quite clear that the activity of DGEBA/NMA in interlayers increased at conditions above 150 °C as shown in Figures 5 and 6. Epoxy network formation in the SE interlayer results in the exfoliation of silicate layers.

Conclusions

The morphology of the natural mica−polymer nanocomposite showed silicate nanolayers with an aspect ratio that is several dozens to hundreds of times greater than conventional exfoliated clay−polymer nanocomposites. In conventional nanocomposites, rigidity, gas barrier properties, and heat resistance increased with an increased exfoliation of clay particles in the polymer matrix. Exfoliated layered silicate−polymer nanocomposites based on delaminated highly crystalline natural micas enabled a system containing dispersed nanolayers with an extremely large aspect ratio. This new composite system could extend the field of high performance materials beyond traditional applications to encompass new unexpected functionalities. Besides its great significance in materials development, similar mechanisms that are involved in the exfoliation behavior of nonexpandable layered silicates in the environment can be applied in nanotechnology. The strengthening mechanisms and barrier properties of this newly created nanocomposite would be further investigated.

Acknowledgment. This research was partially supported by the Ministry of Education, Culture, Sports, Science and Technology (MEXT), Grant-in-Aid for Scientific Research (C), 18550184. The authors are grateful to Mr. Y. Yajima of National Institute for Materials Science (NIMS) for his assistance with wet chemical analysis. We thank Mr. K. Kurashima of the National Institute for Materials Science (NIMS) for technical support in TEM observations. We also thank Dr. A. Yamamoto of the National Institute for Materials Science (NIMS) for the use of ultramicrotome.

CM702860M

(40) Tanaka, Y.; Bauer, R. S. In *Epoxy Resins: Chemistry and Technology*; May, C. A., Ed.; Marcel Dekker: New York, 1988; pp 285–464.